Supplementary Information

Large-scale computational assembly of ionic liquid/MOF composites: synergistic effect in wire-tube conformation for efficient CO_2/CH_4 separation

Youshi Lan, [a] Tongan Yan, [a] Minman Tong, *[b] and Chongli Zhong*[a,c]

[a]State Key Laboratory of Organic-Inorganic Composites, Beijing University of Chemical Technology, Beijing 100029, China.

[b]School of Chemistry and Materials Science, Jiangsu Normal University, Xuzhou 221116, China.

[c]School of Chemistry and Chemical Engineering, Tianjin Polytechnic University, Tianjin 300387, China

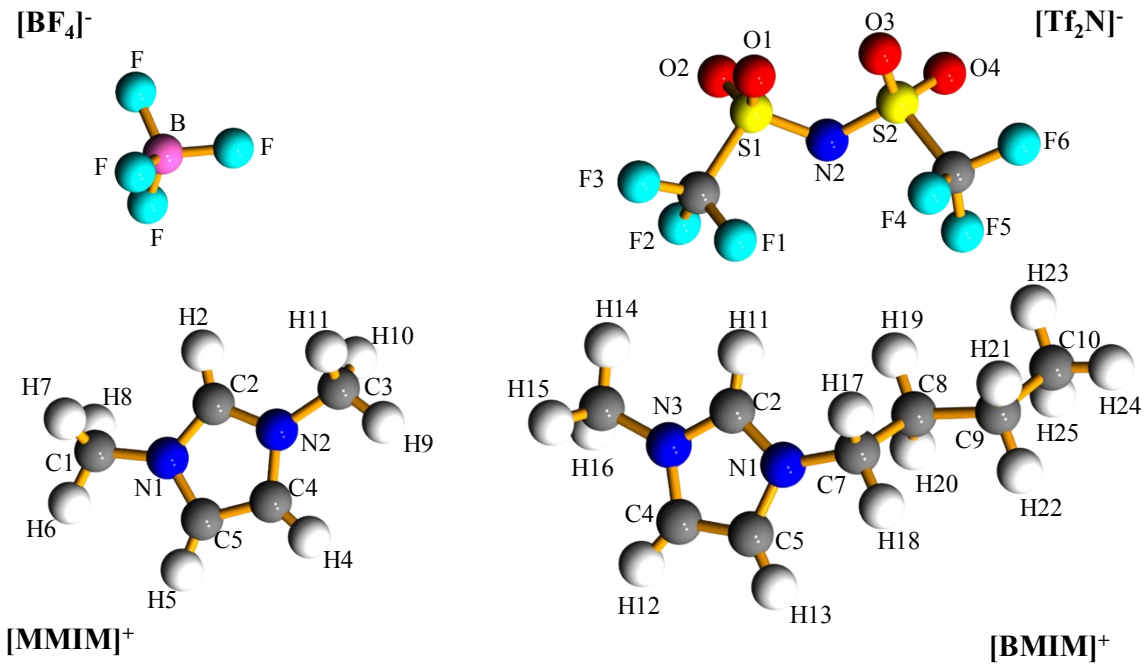

Fig. S1 Configuration of ILs in this work and corresponding atomic IDs.

Table S1. Force field parameters and point charges for the ionic liquids studied in this work.

Atomic IDs	Atomic types	ε/k_B (K)	σ (nm)	q (e)
$[MMIM]^+$				
N1	NA	85.55	0.3250	0.173
C5	CW	43.28	0.3400	-0.198
C4	CW	43.28	0.3400	-0.198
N2	NA	85.55	0.3250	0.173
C2	CR	43.28	0.3400	0.144
C1	CT	55.05	0.3400	0.384
H5	H4	7.55	0.2511	0.238
H4	H4	7.55	0.2511	0.238
C3	CT	55.05	0.3400	0.384
H2	H5	7.55	0.2422	0.256
H8	H1	7.90	0.2471	0.17
H7	H1	7.90	0.2471	0.17
H6	H1	7.90	0.2471	0.17
H10	H1	7.90	0.2471	0.17
H11	H1	7.90	0.2471	0.17
H9	H1	7.90	0.2471	0.17
$[BF_4]^-$				
B	B	47.81	0.3581	1.134
F	F	30.70	0.3118	-0.533

[BMIM]$^+$				
C5	CW	43.28	0.3400	-0.1885
H13	H4	7.55	0.2511	0.2506
C4	CW	43.28	0.3400	-0.1415
H12	H4	7.55	0.2511	0.2324
C2	CR	43.28	0.3400	0.0231
H11	H5	7.55	0.2421	0.2291
N1	NA	85.55	0.3250	0.0077
N3	NA	85.55	0.3250	0.0785
C7	CT	55.05	0.3400	-0.0118
H17	H1	7.90	0.2471	0.0852
H18	H1	7.90	0.2471	0.0852
C6	CT	55.05	0.3400	-0.1489
H14	H1	7.90	0.2471	0.1229
H15	H1	7.90	0.2471	0.1229
H16	H1	7.90	0.2471	0.1229
C8	CT	55.05	0.3400	-0.0464
H19	HC	7.90	0.2650	0.043
H20	HC	7.90	0.2650	0.043
C9	CT	55.05	0.3400	0.0126
H21	HC	7.90	0.2650	0.0237
H22	HC	7.90	0.2650	0.0237
C10	CT	55.05	0.3400	-0.0402
H23	HC	7.90	0.2650	0.0236
H24	HC	7.90	0.2650	0.0236
H25	HC	7.90	0.2650	0.0236
$[Tf_2N]^-$				
C11	C	33.21	0.3500	0.3603
C12	C	33.21	0.3500	0.3369
N2	N	85.55	0.3250	-0.7148
S1	S	125.81	0.3550	1.0227
S2	S	125.81	0.3550	1.0282
O1	O	105.68	0.2960	-0.5576
O2	O	105.68	0.2960	-0.5552
O3	O	105.68	0.2960	-0.5574
O4	O	105.68	0.2960	-0.5559
F1	F	26.67	0.2950	-0.1437
F2	F	26.67	0.2950	-0.1035
F3	F	26.67	0.2950	-0.1655
F4	F	26.67	0.2950	-0.1377
F5	F	26.67	0.2950	-0.0977
F6	F	26.67	0.2950	-0.1592
Bond types		K_b (kcal·mol^{-1}·Å^{-2})		b_0 (nm)

NA-CR	477.00		0.1343
NA-CW	427.00		0.1381
NA-CT	280.11		0.1472
CR-H5	367.00		0.1080
CW-CW	409.89		0.1343
CW-H4	367.00		0.1080
CT-H1	340.00		0.1090
CT-CT	310.00		0.1526
CT-HC	340.00		0.1090
C-F	441.80		0.1323
C-S	235.42		0.1818
S-O	637.07		0.1442
N-S	372.01		0.1570
B-F	289.91		0.1389
Angle types	K_θ (kcal·mol^{-1}·rad^{-2})		θ_0 (º)
CR-NA-CW	70.00		120.00
CR-NA-CT	49.95		126.30
CW-NA-CT	49.95		125.70
NA-CR-NA	70.00		120.00
NA-CR-H5	50.00		120.00
NA-CW-CW	119.98		107.10
NA-CW-H4	50.00		120.00
CW-CW-H4	30.11		130.70
NA-CT-H1	54.97		109.50
NA-CT-CT	70.03		112.20
H1-CT-H1	35.00		109.50
CT-CT-H1	50.00		109.50
CT-CT-CT	40.00		109.50
HC-CT-HC	35.00		109.50
CT-CT-HC	50.00		109.50
F-C-F	93.33		107.10
S-C-F	82.93		111.80
C-S-O	103.97		102.60
O-S-O	115.80		118.50
O-S-N	94.29		113.60
C-S-N	97.51		100.20
S-N-S	80.19		125.60
F-B-F	49.95		109.50
Dihedral types	K_φ (kcal·mol^{-1})	n	φ_0 (º)
CT-CT-CT-CT	0.18	3	0.00
CT-CT-CT-NA	0.25	3	0.00
CT-CT-CT-HC	0.16	3	0.00
CT-CT-CT-H1	0.16	3	0.00

NA-CT-CT-HC	0.16	3	0.00
HC-CT-CT-HC	0.15	3	0.00
HC-CT-CT-H1	0.16	3	0.00
CT-CT-NA-CW	-0.18	1	0.00
CT-CT-NA-CR	-0.24	1	0.00
H1-CT-NA-CW	0.24	3	0.00
H1-CT-NA-CR	0.16	3	0.00
NA-CW-CW-NA	12.00	2	180.00
NA-CW-CW-H4	1.50	2	180.00
CW-CW-NA-CT	2.00	2	180.00
CW-CW-NA-CR	12.00	2	180.00
H4-CW-NA-CT	1.50	2	180.00
H4-CW-NA-CR	2.00	2	180.00
NA-CR-NA-CT	2.00	2	180.00
NA-CR-NA-CW	12.00	2	180.00
H5-CR-NA-CT	1.50	2	180.00
H5-CR-NA-CW	1.50	2	180.00
Dihedral types	V_1 (kcal·mol^{-1})	V_2 (kcal·mol^{-1})	V_3 (kcal·mol^{-1})
F-C-S-O	0.00	0.00	0.35
S-N-S-O	0.00	0.00	0.00
F-C-S-N	0.00	0.00	0.32
S-N-S-C	7.83	-2.49	-0.76
Improper types	K_ψ (kcal/mol)	n	ψ_0 (°)
CR-CW-NA-CT	2.00	2	180.00
H4-CW-NA-CW	1.10	2	180.00
H5-CR-NA-NA	1.10	2	180.00

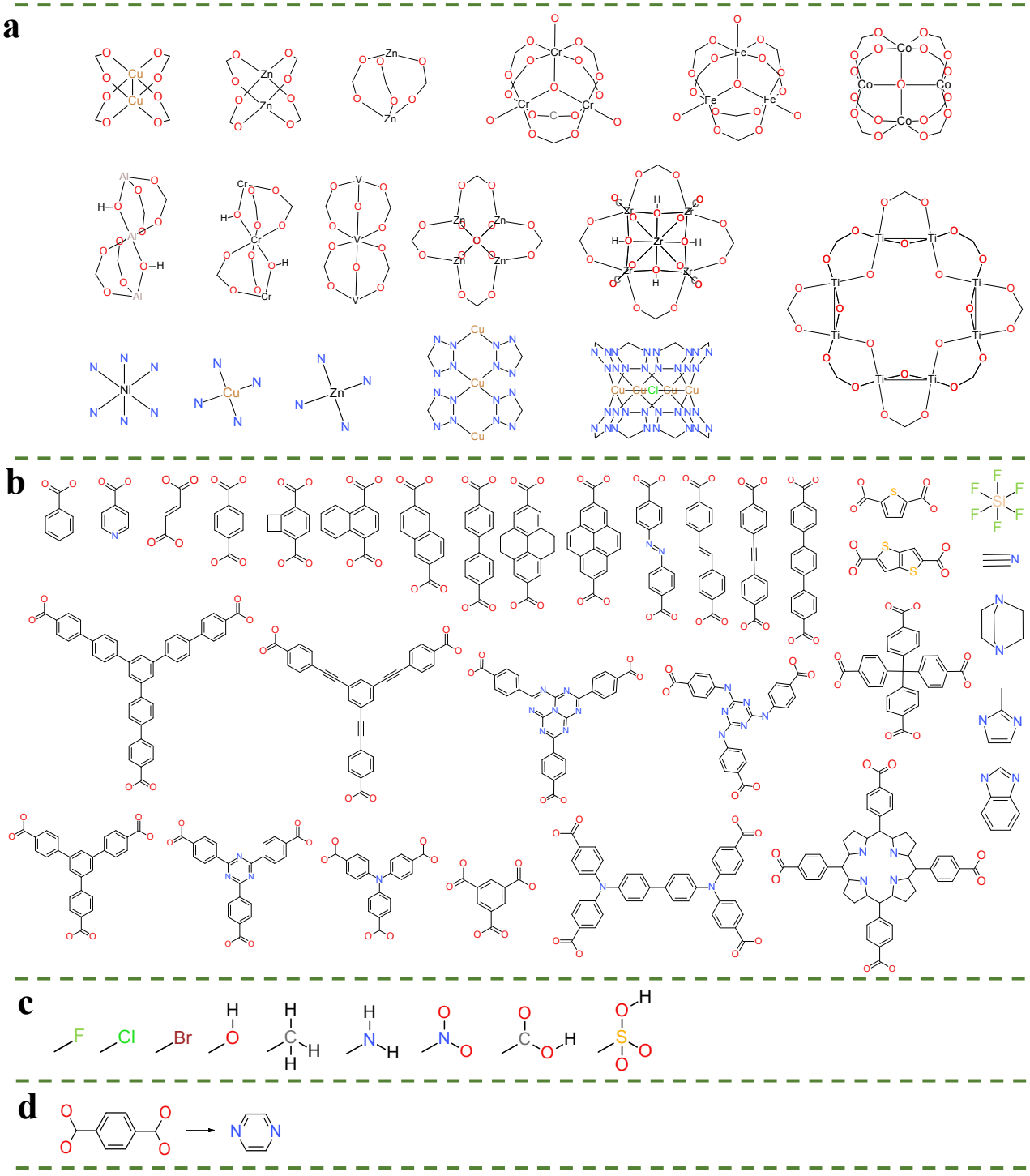

Fig. S2 Full list of the primary units used to generate the database of MOFs. a, 17 metal clusters. **b**, 32 organic linkers. **c**, 9 functional groups. **d,** the carboxylate connection site of all the organic primary units here can be replaced by the nitrogen atom for pyridine connection

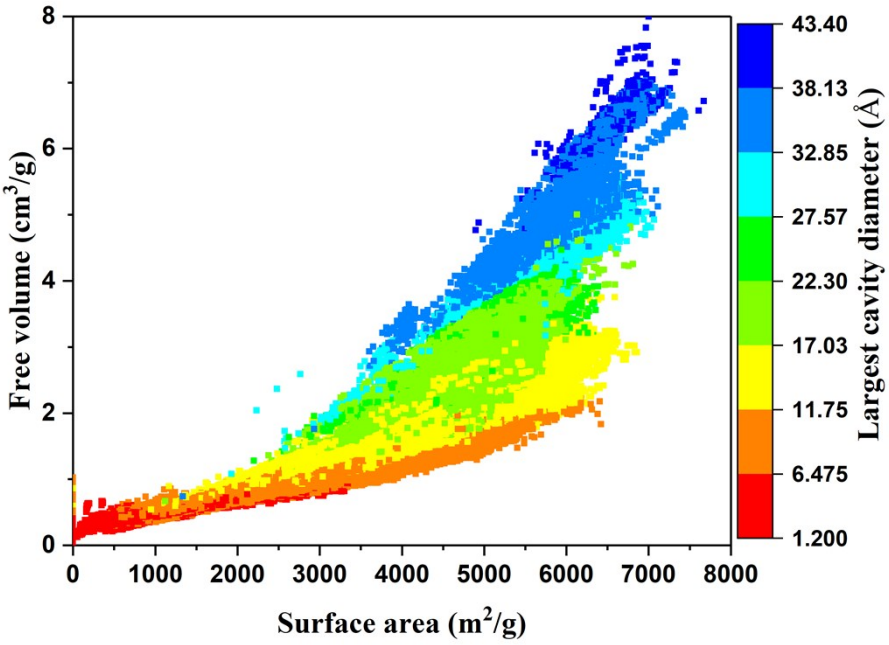

Fig. S3 Relationship between the surface area and free volume of the generated MOFs in our database, colored by material largest cavity diameter.

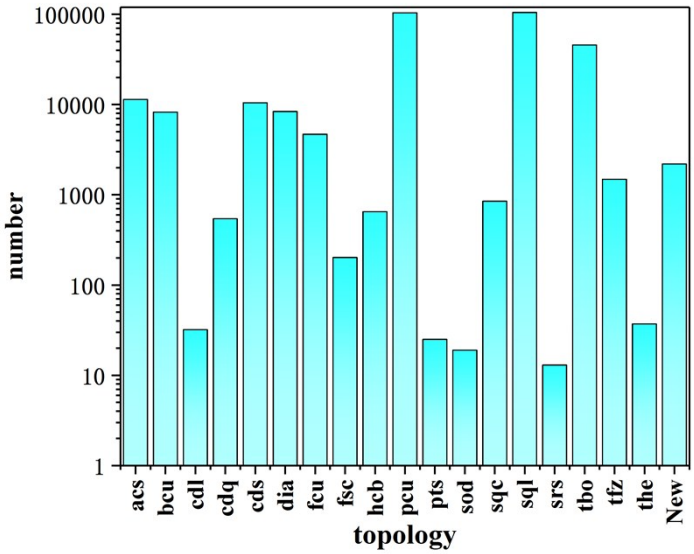

Fig. S4 Topology distribution of generated MOF database.

Table S2. Comparison of the structural energy and CO_2/CH_4 separation performance of the CBMC- and MD- derived [MMIM][BF_4]/MOF composites.

MOFs	CBMC			MD		
	E **(kcal/mol)**	S_{CO_2/CH_4}	N_{CO_2} **(mmol/g)**	***E*** **(kcal/mol)**	S_{CO_2/CH_4}	N_{CO_2} **(mmol/g)**
Cu-BTC	-832.26	11.64	3.73	-849.16	12.15	4.02
IRMOF-1	-861.63	11.99	2.64	-895.84	10.74	2.28
MIL-68Al	-2799.33	16.00	6.54	-2795.92	17.50	6.79
UiO-66	-3972.63	19.25	2.90	-3927.95	22.16	3.12
ZIF-8	-783.78	6.21	2.36	-792.24	6.61	2.49

Table S3. Comparison of the structural energy and CO_2/CH_4 separation performance of the CBMC- and MD- derived [BMIM][Tf_2N]/MOF composites.

MOFs	CBMC			MD		
	E **(kcal/mol)**	S_{CO_2/CH_4}	N_{CO_2} **(mmol/g)**	***E*** **(kcal/mol)**	S_{CO_2/CH_4}	N_{CO_2} **(mmol/g)**
Cu-BTC	1373.31	5.55	2.00	1388.96	5.54	2.04
IRMOF-1	1373.76	3.65	0.74	1382.66	4.96	1.06
MIL-68Al	3182.50	7.57	3.09	3219.48	7.34	3.20
UiO-66	4822.06	9.49	1.13	4805.68	8.99	1.07
ZIF-8	1349.31	3.33	1.08	1347.40	3.64	1.20

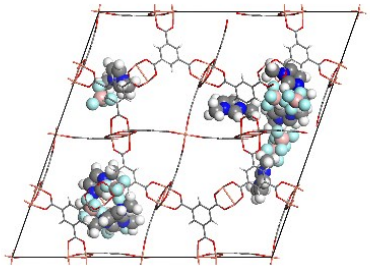

[MMIM][BF_4]/Cu-BTC, CBMC

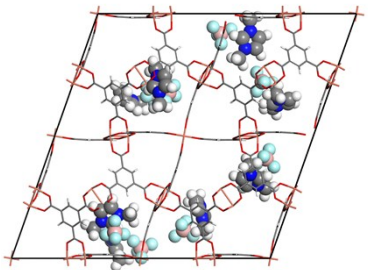

[MMIM][BF_4]/Cu-BTC, MD

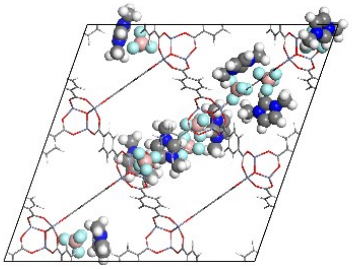

[MMIM][BF_4]/IRMOF-1, CBMC

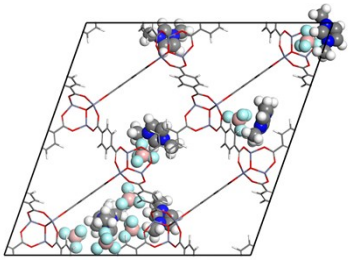

[MMIM][BF_4]/IRMOF-1, MD

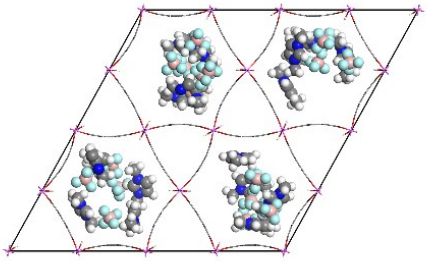

[MMIM][BF_4]/MIL-68Al, CBMC

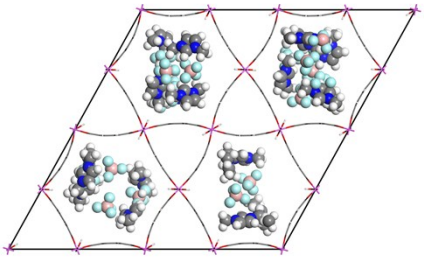

[MMIM][BF_4]/MIL-68Al, MD

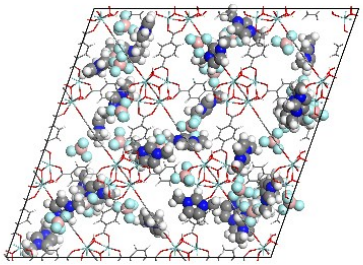

[MMIM][BF_4]/UiO-66, CBMC

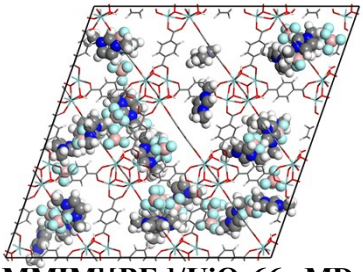

[MMIM][BF_4]/UiO-66, MD

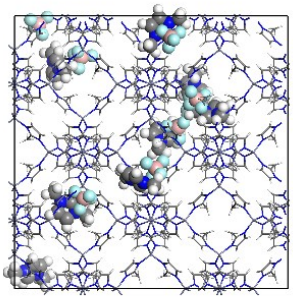

[MMIM][BF_4]/ZIF-8, CBMC

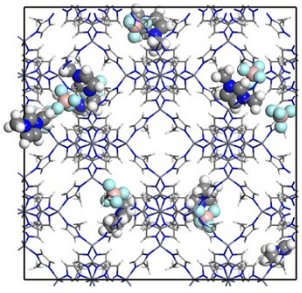

[MMIM][BF_4]/ZIF-8, MD

Fig. S5 Configurations of CBMC- and MD- derived [MMIM][BF_4]/MOFs.

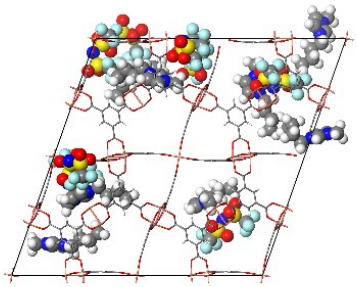

[BMIM][Tf_2N]/Cu-BTC, CBMC

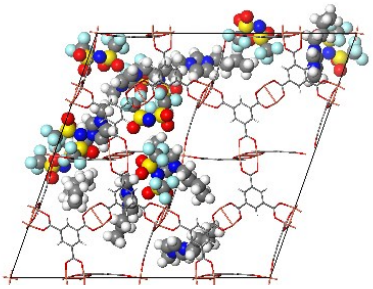

[BMIM][Tf_2N]/Cu-BTC, MD

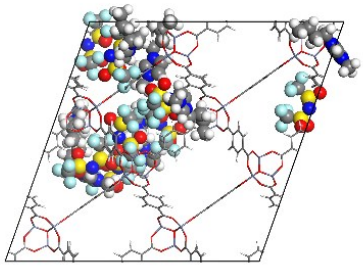

[BMIM][Tf_2N]/IRMOF-1, CBMC

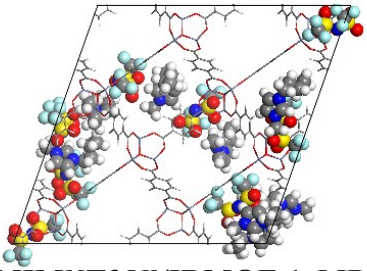

[BMIM][Tf_2N]/IRMOF-1, MD

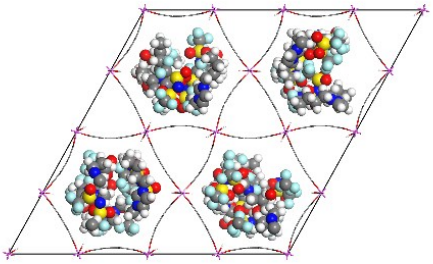

[BMIM][Tf_2N]/MIL-68Al, CBMC

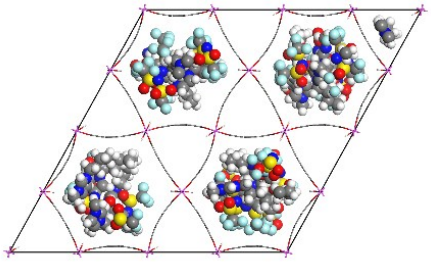

[BMIM][Tf_2N]/MIL-68Al, MD

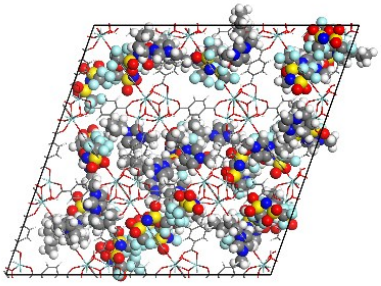

[BMIM][Tf_2N]/UiO-66, CBMC

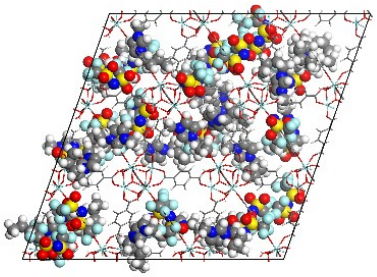

[BMIM][Tf_2N]/UiO-66, MD

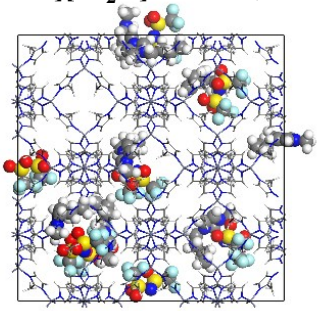

[BMIM][Tf_2N]/ZIF-8, CBMC

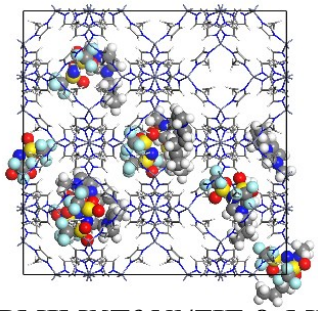

[BMIM][Tf_2N]/ZIF-8, MD

Fig. S6 Configurations of CBMC- and MD- derived [BMIM][Tf_2N]/MOFs.

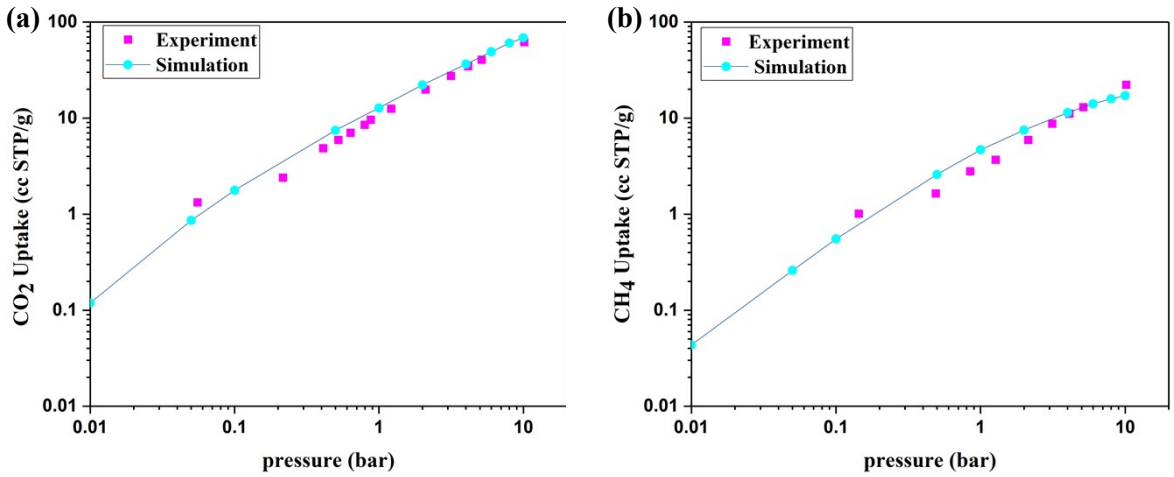

Fig. S7 Gas uptake of [BMIM][BF_4]/ZIF-8 composite from experimental results[1] and GCMC simulations. (a) [BMIM][BF_4] amount of 25 wt% for CO_2 and (b) [BMIM][BF_4] amount of 28 wt% for CH_4. The simulation data is multiplied by the same pressure-dependent factor used in the reported work.

Table S4. CO_2/CH_4 separation performance and geometrical features of the top 2 [BMIM][Tf_2N]/MOF composites and the corresponding original MOFs.

Structure name	S_{CO_2/CH_4}	N_{CO_2} (mmol g^{-1})	PLD (Å)	LCD (Å)	S_{acc} (m^2 g^{-1})	V_f (cm^3 g^{-1})
Zn_2O_8-BTC_B-irmof7_A_No16	44.5	7.6	4.3	6.1	1674.0	0.64
[BMIM][Tf_2N]/ Zn_2O_8-BTC_B-irmof7_A_No16	50.5	4.0	4.3	6.1	163.1	0.40
$Zn_2O_8N_2$-irmof8_A-TePM_No117	37.7	7.4	4.9	5.61	1688.4	0.59
[BMIM][Tf_2N]/ $Zn_2O_8N_2$-irmof8_A-TePM_No117	43.9	4.5	4.9	5.61	687.5	0.43

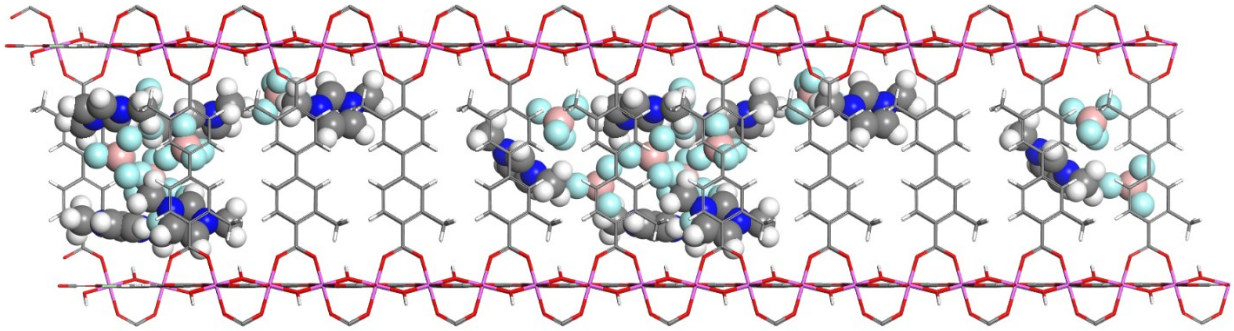

Fig. S8 Representative configuration of IL incorporated in **sql-**MOFs with PLD larger than 10 Å.

Reference

1. B. Koyuturk, C. Altintas, F. P. Kinik, S. Keskin and A. Uzun, *J. Phys. Chem. C*, 2017, 121, 10370-10381.